

Optical Imaging of Calcium Transients in Neurons and Pharyngeal Muscle of *C. elegans*

Neurotechnique

Rex Kerr,* Varda Lev-Ram,[§] Geoff Baird,[†]
Pierre Vincent,^{§#} Roger Y. Tsien,^{†§}
and William R. Schafer^{*||}

*Department of Biology

[†]Biomedical Sciences Graduate Program

[‡]Howard Hughes Medical Institute

[§]Department of Pharmacology
University of California, San Diego
La Jolla, California 92093

Summary

Electrophysiology and optical indicators have been used in vertebrate systems to investigate excitable cell firing and calcium transients, but both techniques have been difficult to apply in organisms with powerful reverse genetics. To overcome this limitation, we expressed cameleon proteins, genetically encoded calcium indicators, in the pharyngeal muscle of the nematode worm *Caenorhabditis elegans*. In intact transgenic animals expressing cameleons, fluorescence ratio changes accompanied muscular contraction, verifying detection of calcium transients. By comparing the magnitude and duration of calcium influx in wild-type and mutant animals, we were able to determine the effects of calcium channel proteins on pharyngeal calcium transients. We also successfully used cameleons to detect electrically evoked calcium transients in individual *C. elegans* neurons. This technique therefore should have broad applications in analyzing the regulation of excitable cell activity in genetically tractable organisms.

Introduction

Genetically tractable model organisms have many advantages for investigating nervous system function at the molecular and cellular levels. For example, the nematode *Caenorhabditis elegans* has a simple and well-characterized nervous system, consisting of only 302 neurons of defined position, connectivity, and cell lineage. Since each neuron can be positively identified based on its position, it is possible to evaluate the function of an individual neuron or group of neurons through single cell laser ablation. Moreover, because of their short generation time, small genome size, and accessibility to germline transformation, *C. elegans* is highly amenable to molecular and classical genetics. Thus, in *C. elegans*, it is relatively easy to identify genes involved in specific behaviors and to infer the functions of their products in the neurons and muscle cells controlling those behaviors using genetics and molecular cloning. To rigorously determine how a particular gene product

affects the activity of an excitable cell, it is often important to directly measure its effect on cellular physiology. Unfortunately, the small neurons and hydrostatic skeleton of *C. elegans* have made physiological studies difficult, especially in live animals. Existing protocols for recording electrically from *C. elegans* neurons or muscle cells all involve slicing open or rupturing the cuticle to expose the cell of interest, and recordings from intact behaving animals have not been reported. In principle, calcium imaging offers an alternative approach for monitoring excitable cell activity in vivo. However, the anatomy of *C. elegans* presents a number of difficulties for using traditional dyes for calcium imaging. The relatively impermeant cuticle prevents uptake of bath-applied dye, and the hydrostatic skeleton makes dissection and microinjection difficult. Although large cells, such as oocytes and intestinal cells, have been successfully loaded with calcium-sensitive dye through microinjection, neurons and even many muscle cells are too small to reliably load in this way. Moreover, even when successful, microinjection has been limited to single cells (Dal Santo et al., 1999).

To circumvent these problems, we are using the calcium indicator protein cameleon (Miyawaki et al., 1997) to image calcium transients in intact *C. elegans*. Cameleons are composed of four domains: cyan fluorescent protein (CFP), calmodulin, M13 (a calmodulin binding domain), and yellow fluorescent protein (YFP). In low calcium concentrations, calmodulin is not bound to M13, and the protein is in a poor configuration for fluorescence resonance energy transfer (FRET) between CFP and YFP. Excitation of CFP leads primarily to CFP emission, with lesser energy transfer to YFP and YFP emission. Upon an increase in calcium concentration, calmodulin binds calcium and attracts M13. This brings CFP and YFP into a more favorable location or orientation for FRET; excitation of CFP will then lead to increased energy transfer and an increase in YFP emission at the expense of CFP emission. Hence, an increase in calcium causes an increase in the YFP/CFP fluorescence intensity ratio. The ratiometric nature of the indicator is ideal for in vivo application to moving cells, as motion artifacts that affect total intensity are cancelled out in the ratio. Genetically encoded sensors, such as cameleon, are especially attractive for organisms such as *C. elegans*, in which a large number of tissue-specific promoters are known. In addition to allowing precise tissue targeting and reducing the effort required to prepare each animal, subcellular localization can be achieved by using appropriate signal sequences attached to the sensor.

Cameleons were previously shown to function as a fluorescent calcium sensor in cultured cells. To develop methods for using cameleon in an intact animal, we chose to concentrate primarily on the pharyngeal muscle of *C. elegans*. The pharynx is a relatively large (around 20 μm in diameter at the terminal bulb) muscular organ that pumps bacteria into the worm's intestine for

^{||} To whom correspondence should be addressed (e-mail: wschafer@ucsd.edu).

[#] Present address: Neurobiologie Cellulaire, CNRS UMR 7624, Paris, France.

consumption. The pharynx pumps rapidly in the presence of serotonin, and calcium transients can be independently detected through the visible contraction of the muscle cells. Electrical recordings have been made from the dissected pharyngeal muscles of wild-type and mutant worms, making the pharynx perhaps the physiologically best-characterized excitable tissue in *C. elegans* (Avery and Thomas, 1997). Since many of the components involved in production and regulation of calcium transients are common to both muscles and neurons, an investigation of molecular function in muscles may aid in understanding neuronal calcium dynamics. However, the calcium dynamics of the pharynx have not been explicitly studied, due largely to a lack of appropriate calcium sensors.

Here, we describe the use of cameleon to image calcium transients in the excitable cells of *C. elegans*. We have detected calcium influx in the pharyngeal muscle of intact animals as part of normal feeding behavior, and in neurons, in response to an extracellular electrical stimulation. Imaging studies of mutant animals provided insight into the effects of calcium channel proteins on the calcium dynamics of *C. elegans* muscle cells.

Results

Detection of Pharyngeal Calcium Transients in *C. elegans*

To verify that cameleon could be used to detect calcium transients in the *C. elegans* pharynx, we created an expression vector driving the YC2.1 (yellow cameleon 2.1) variant of cameleon (Miyawaki et al., 1999) in the *C. elegans* pharynx under the control of the pharyngeal specific *myo-2* promoter (Okkema et al., 1993). We then created a line of worms containing an integrated array of this expression vector. The *ljls1* line showed moderately variable expression levels of YC2.1 throughout the pharynx. Typically, the terminal bulb had the highest expression, while the corpus had lower expression levels. Fluorescence was frequently not visible in the isthmus. A typical example of expression in the pharynx is shown in Figure 1B.

We recorded from adult hermaphrodite worms from the *ljls1* line. Feeding behavior was stimulated by exposure to serotonin (Avery and Horvitz, 1990). We used a MultiViewer (Princeton Instruments), a wide-field emission image splitter, to make simultaneous measurements of both the cyan and yellow emission intensities with a single CCD camera, as diagrammed in Figure 1A. The cyan-filtered image fell on the top half of the CCD array, while the yellow-filtered image fell on the bottom half, yielding raw images like the one shown in Figure 1B. The split images were superimposed, aligned, and displayed with the software package MetaFluor (Universal Imaging). A color scale was used to indicate the ratio at each pixel and assist in visual identification of fluorescence ratio changes. Frames showing visible opening of the terminal bulb (caused by muscular contraction) also showed elevated fluorescence emission ratios, consistent with elevated calcium during contraction (Figures 1C and 1D).

To follow calcium transients over time, we recorded streams of images at 20 Hz and calculated the mean fluorescent intensity ratio over the terminal bulb of the

pharynx. As shown in Figure 2A, traces of the mean ratio in terminal bulb showed distinct peaks during active pumping. Observation of contractile events showed that the onset of visible contraction occurred simultaneously with the increase in fluorescence ratio (Figure 2A). To verify that the ratio changes were a result of calcium influx and not motion artifacts, we artificially induced motion artifacts by changing the focal plane and moving the stage during recording. Ratio changes were minimal and differed in appearance from the sharp rises accompanying pharyngeal contraction. The slow return to baseline in the ratio signal was also inconsistent with any movement artifacts. Finally, we liberated the worms' heads from their bodies and applied digitonin, a membrane-permeabilizing detergent, to gain access to the cytoplasm of the pharynx. External application of intracellular saline with either 0 Ca^{2+} + 4 mM EGTA or 10 mM Ca^{2+} gave a ratio change of $72\% \pm 4\%$ (Figure 2C), reasonably consistent with the maximum ratio change of 90%–100% in vitro (Miyawaki et al., 1999). Thus, the cameleon protein expressed within the pharynx showed normal responses to calcium. Taken together, these results indicated that the observed increases in ratio were reliably indicating calcium transients within the muscle.

The ability to effectively image calcium transients in the pharynx was affected by a number of technical considerations. First, ratiometric imaging appeared to be critical for reliable detection of calcium changes. Although it was frequently possible to infer the location of the contractions from an individual wavelength trace, the ratioing process removed a great deal of the noise resulting from sample movement and photobleaching (Figure 2B). Second, while gluing was effective at keeping the worm in the field of view, it was often not sufficient to completely immobilize the head without adversely affecting behavior. This problem could be overcome by manually updating a fixed region of interest each time the worm moves so that the region is always appropriately centered. However, manual tracking greatly limits the number of traces that can be analyzed and may introduce artifacts when comparing strains of worms that move more or less do than wild type. We therefore developed software to automatically track regions of interest while maintaining the proper offset between the two wavelength regions, which reduced noise (mean fluctuation during periods when there was no muscle contraction) to under a 0.1% ratio change in most cases. Third, since cameleon is based on the endogenous calcium binding protein calmodulin, there is concern about cameleon expression affecting behavior. We were unable to distinguish wild-type worms from those with *ljls1* on the basis of observing pharyngeal pumping, and *ljls1* animals did not have a starved appearance. We therefore concluded that the effect of cameleon expression on pharyngeal pumping behavior is minor. Photobleaching did not present technical problems; the loss of intensity was minor (<5% in 10 s), and recovery was rapid enough to allow us to record for as long as the worm survived on the pad (up to 5 hr, recording 10 s/min).

The appearance of the ratio traces raised questions about relationship between the fluorescence ratio of cameleon and the calcium dynamics of the pharynx. We observed that it took much longer for the ratio to return to baseline than for the muscle to contract; a rapid series

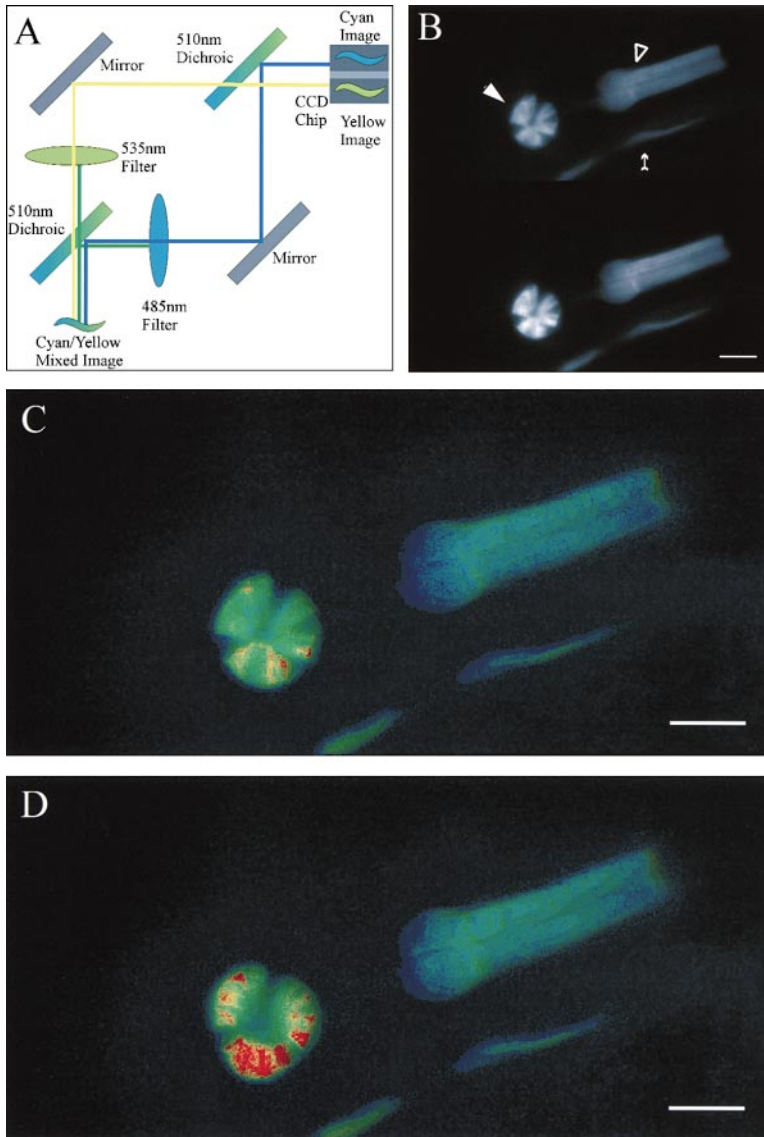


Figure 1. Imaging of Cameleon in the *C. elegans* Pharynx

(A) Simultaneous dual emission recording with an emission image splitter. The emitted light is split with a dichroic mirror, and cyan and yellow channels are isolated with filters, then recombined with a small offset and projected onto a single CCD chip.

(B) An unprocessed image of the pharynx under 405 nm excitation. The top image is the cyan (485 nm) channel; the bottom image is the yellow (535 nm) channel. The terminal bulb (closed arrowhead) was used for subsequent analysis. The corpus (open arrowhead) often also showed expression. Reflections off of bubbles (small arrow) were ignored. The worm's nose is to the upper right; the remainder of the body leaves the field of view to the lower left. Scale bar, 20 μm .

(C) A split and aligned image of the pharynx when the muscle is not contracted. Color indicates the intensity of yellow over the intensity of cyan for each pixel; red hues indicate high ratios, or higher calcium, while blue hues indicate lower ratios, or lower calcium. Brightness reflects mean intensity of the pixels in each channel. Scale bar, 20 μm .

(D) Image of the same worm while the pharynx is contracted. There is a marked red shift in the pseudocolor image of the contracted image relative to the uncontracted one, as expected from an increase in calcium levels. Scale bar, 20 μm .

of contractions could cause the ratio to become significantly elevated from baseline. However, in worms expressing YC3.1, a cameleon with lowered affinity for calcium relative to YC2.1 (Miyawaki et al., 1997), the ratio changes were smaller and returned to baseline more rapidly (Figure 2D). One explanation for these observations is that the higher affinity of YC2.1 allows it to bind a larger fraction of the total calcium and lowers free calcium to the point at which natural calcium export and sequestration mechanisms are affected. This would cause YC2.1 to have a larger ratio change, with a slower decay back to baseline, as is observed. Alternatively, the difference in rate might be a consequence of YC2.1 having slower kinetics of calcium release than does YC3.1. Preliminary *in vitro* experiments in which calcium-saturated cameleons were rapidly mixed with EDTA verified that YC2.1 had an ~ 2 -fold slower off rate than did YC3.1. These experiments also indicated that release kinetics of both cameleons were at least biexponential, with a rapid release phase of $\sim 100 \text{ s}^{-1}$ that was not observed in worm imaging. Furthermore, the cyan

and yellow channels had somewhat different slow phase rate constants (cyan: $4.7 \pm 0.2 \text{ s}^{-1}$, yellow: $2.6 \pm 0.1 \text{ s}^{-1}$ for YC2.1; cyan: $8.8 \pm 0.3 \text{ s}^{-1}$, yellow $5.1 \pm 0.1 \text{ s}^{-1}$ for YC3.1), suggesting that a portion of the fluorescence change could be due to a conformational alteration of YFP or CFP rather than a change in FRET. Since accurate kinetic data are essential for determining exact calcium levels but not for making quantitative comparisons between different fluorescence ratio measurements, we did not pursue a detailed investigation of cameleon kinetics. We have not yet attempted to analyze the decay phase, given the difficulty of determining which factors were contributing to the observed shape. For our analysis of the rising phase, we continued to use YC2.1 in order to maximize our signal.

Evoked Ratio Changes in *C. elegans* Neurons

To image calcium transients in neurons, we used the array *ljEx3*, which expresses YC2.1 under the control of the panneuronal *unc-119* promoter (Maduro and Pilgrim,

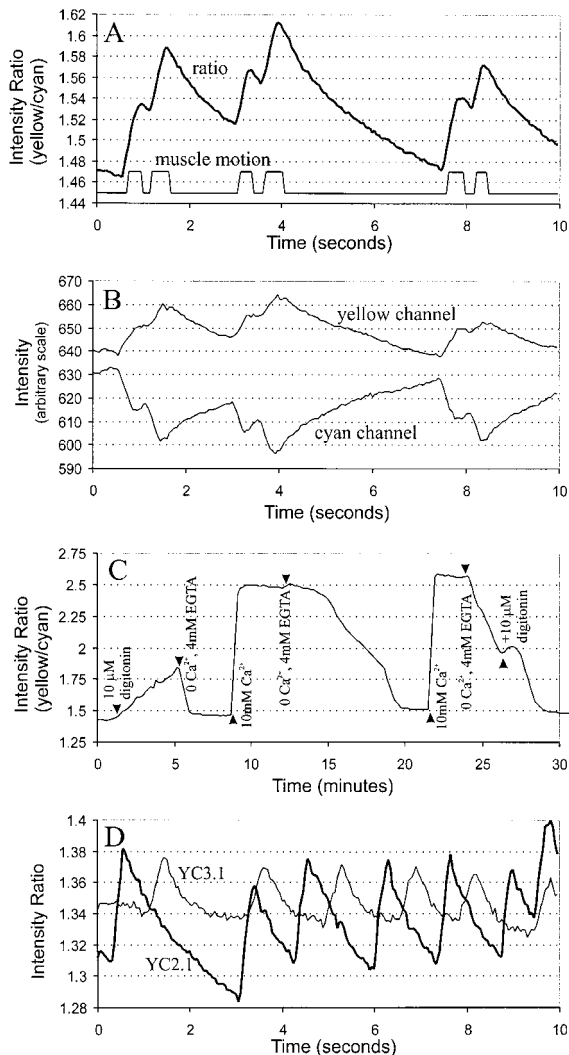


Figure 2. Visualization of Calcium Transients

(A) The yellow/cyan intensity ratio (thick line) over the terminal bulb of the pharynx shows rapid rises followed by slower decays; the rises are accompanied by muscular contraction (thin line), indicating that they are caused by a rise in calcium.

(B) The yellow and cyan channels separately show a relative reduction in cyan and increase in yellow intensity with contraction, as expected. However, each individual channel is affected by motion artifact noise, in contrast to the ratio in (A).

(C) Calibration of cameleon. A dissected head was exposed to the membrane-permeant digitonin to give intracellular access and then exposed to solutions of 10 mM calcium or 4 mM EGTA to determine the maximum and minimum ratio. A typical trace is shown here. The maximum/minimum ratio change was $72\% \pm 4\%$ averaged over five worms. Arrowheads indicate solution changes.

(D) Comparison of YC2.1 with YC3.1 in worms pumping at the same rate. The rate of decay is faster for YC3.1 (thin line) than for YC2.1 (thick line), most apparent in the sharp transition between descending and rising ratios in YC2.1, which is more rounded in YC3.1, and indicative of a return to near baseline for YC3.1 but not YC2.1 at the rate shown. This is consistent with faster in vitro kinetics for YC3.1 and sensitivity to lower calcium levels for YC2.1.

1995), as shown in Figure 3A. Application of external calcium in a membrane-permeabilized preparation showed that neuronally expressed cameleon was responsive to

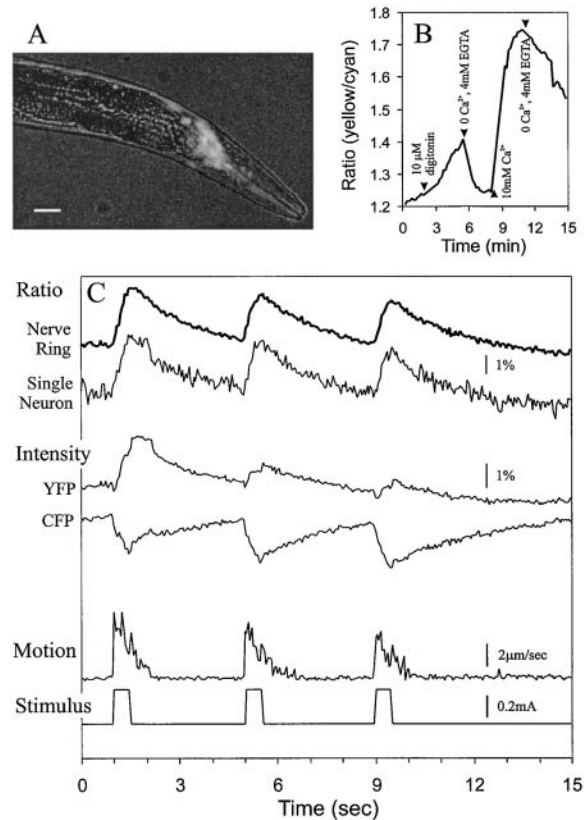


Figure 3. Preliminary Investigation of Neuronal Calcium Transients (A) Expression pattern of YC2.1 under the *unc-119* promoter. Fluorescence is most noticeable in the nerve ring clustered around the pharynx in the head, though expression patterns and intensity vary from worm to worm. The image shows merged fluorescence and transmitted light. The worm's head is to the lower right. Scale bar, 20 μm .

(B) Cameleon retains activity in *C. elegans* neurons. The head of a *ljEx3* worm was removed, exposed to the detergent digitonin, and switched between calcium-free (4 mM EGTA) solution and 10 mM calcium solution to determine the maximal response of cameleon in neurons. Although intracellular access to all neurons in the field of view may not be uniform, neuronal cameleon is clearly responsive to calcium changes. Arrowheads indicate solution changes.

(C) Response of neurons to electrical stimulation. Both the entire nerve ring (top trace) and individual neurons within the nerve ring (second trace) show transient increases in fluorescent ratio coupled to electrical stimulation (bottom trace; each stimulus consists of a train of 100 0.1 ms current pulses at 200 Hz). The individual wavelengths (middle two traces) show roughly opposite changes in intensity over the entire nerve ring, as expected for a change in FRET, though both traces have significantly increased noise, especially during periods of motion caused by muscle contraction (second to bottom trace). Intensities were corrected for photobleaching by removing the exponential trend before and after stimulation; without correction, the YFP channel decreased by $\sim 10\%$ during the recording.

calcium (Figure 3B), although noise levels were increased by an order of magnitude or more due to the small size of *C. elegans* neurons. Use of a video rate two-photon microscope (Fan et al., 1999) decreased the background fluorescence from neighboring neurons, which would dilute any signal, but did not decrease noise levels a great deal.

We next investigated whether cameleon could be used to detect voltage-dependent calcium transients in live neurons. A survey of neurons in intact worms showed occasional small ratio changes that were not immediately attributable to motion artifacts. However, since there are no independent indicators of neuronal activity in *C. elegans* that work in behaving animals, we were unable to verify that any ratio changes seen in such animals were a result of neuronal activity and not artifactual. Therefore, to verify that cameleon could detect authentic neuronal calcium transients, we used an extracellular glass electrode to induce activity through electrical stimulation. The electrode was used to pierce the worm's cuticle and was positioned in close proximity to neurons in the nerve ring. Electrical stimulation produced ratio changes in ring neurons, as shown in Figure 3C. Although activity was synchronous throughout the nerve ring, transients in individual neurons were large enough to be detectable. The electrical stimulation caused muscle contraction that created motion in the sample, causing additional noise in the individual wavelength intensities that was roughly correlated with the motion. In instances in which motion of the sample made the individual wavelengths difficult to interpret, such as was the case for the single neuron trace in Figure 3C, the ratio changes nonetheless appeared very similar to those cases in which motion effects were minor. This indicates the value of the ratiometric nature of the indicator in a moving sample.

Quantitative Monitoring of Pharyngeal Calcium Transients

We next investigated whether we could quantitatively measure the duration and magnitude of calcium transients in the pharynx. We developed software to automatically extract mean ratio traces from stacks of images of a worm's terminal bulb and to calculate the duration, total increase, and rate of increase for the rising phase of each calcium transient (Figure 4A). To interpret these parameters, we first investigated whether calcium buffering by cameleon needed to be corrected for. Although the dye concentration, as assayed by fluorescence intensity, varied by more than a factor of two between worms, we saw essentially no correlation between fluorescent intensity and the magnitude of changes (data not shown). This observation is consistent with the free calcium during calcium influx being set by endogenous buffers, with relatively little impact from cameleon. We then attempted to determine whether the slope or the magnitude of the transients was more indicative of calcium influx levels. The rising phase of the transients is approximately linear with time in most cases (Figure 4A), which means that longer transients will have a greater magnitude simply by virtue of being longer. Two simple hypotheses can explain the approximately linear increase. The influx of calcium could lead to a steady increase in free calcium levels, in which case a greater influx would cause a more rapid increase, causing an increase in slope. Alternatively, the free calcium levels could be approximately constant during the transient, and the steady increase could be an indication of the calcium binding rate of cameleon; greater calcium influx in this case would alter free calcium levels, increasing the binding rate. Fortunately,

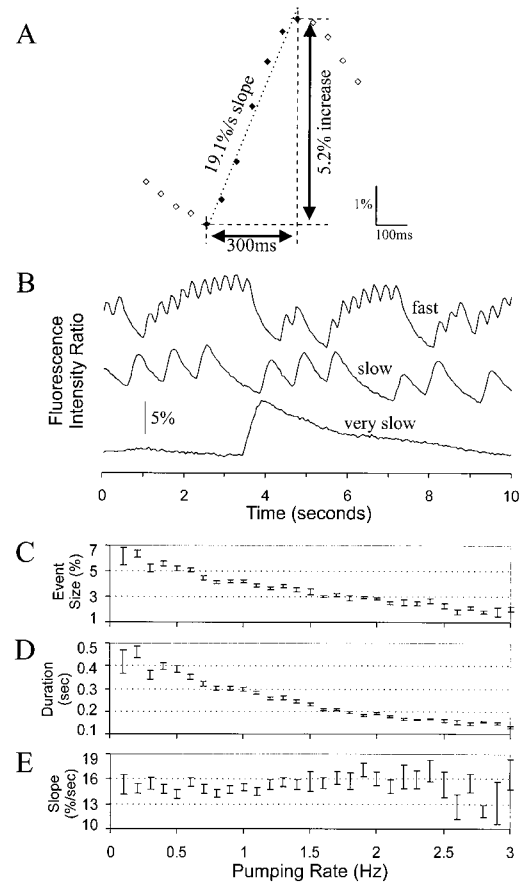


Figure 4. Characterization of Dependence of Calcium Transients on Worm Behavior

(A) Illustration of measured parameters for each transient. Duration is in multiples of the frame rate. Total increase is expressed in percent change in ratio. Rate of increase is computed by a least-squares fit to the rising slope and has units of (percent change in ratio)/(time).
 (B) Sample traces indicating fluorescence ratio traces typical of "fast" (>1.5 Hz), "slow" (0.5–1.5 Hz), and "very slow" (<0.5 Hz) pumping behavior. Note that duration and total increase of transients are dependent on the pumping rate.
 (C) Total ratio increase during transients is reduced at higher pumping rates. Ratio increase is calculated separately for each 0.1 Hz increment in pumping rate; error bars indicate standard error at that rate. The linear correlation coefficient of pumping rate and total increase is -0.66 .
 (D) Total duration of transients is reduced at higher pumping rates. Data points and error bars are computed as in (C). The linear correlation coefficient of pumping rate and duration is -0.67 .
 (E) Slope of ratio increase during transients is relatively unaffected by pumping rate. Data points and error bars are computed as in (C). The linear correlation coefficient of pumping rate and slope is $+0.05$.

although it is difficult to distinguish these two effects, both indicate that the slope of the transients is a monotonic increasing function of the calcium influx. This is sufficient to rank mutants in order of calcium influx.

Using our analysis software, we categorized the wild-type feeding behavior roughly into "fast" pumping (>1.5 Hz), "slow" pumping (0.5–1.5 Hz), or "very slow" pumping (<0.5 Hz), as shown in Figure 4B. Previous studies (Avery and Horvitz, 1989; Raizen et al., 1995) have shown

Table 1. Parameters for Calcium Transients during Pharyngeal Pumping for Wild Type and Mutants

Strain	Pumping Rate	Transient Parameters		
		Duration	Ratio Increase	Slope
N2 (wild-type)	1.16 ± 0.08 Hz	295 ± 10 ms	4.31 ± 0.16%	15.9 ± 0.8%/s
Percentage difference from wild type				
<i>egl-19(n2368)</i>	0.60 ± 0.09 Hz**	+17.7% ± 5.6%*	+18.8% ± 9.0%	-13.9% ± 4.3%*
<i>egl-19(ad695)</i>	1.12 ± 0.12 Hz	+14.0% ± 7.0%◇	+18.0% ± 9.0%*	-4.6% ± 7.9%
<i>egl-19(n582)</i>	0.71 ± 0.08 Hz**	+5.4% ± 5.2%	+3.4% ± 8.3%	+5.9% ± 7.3%
<i>egl-19(ad1006)</i>	1.20 ± 0.11 Hz	-12.6% ± 7.0%◇	-19.4% ± 7.0%*	-13.3% ± 2.6%
<i>unc-36(e251)</i>	0.58 ± 0.09 Hz**	+1.2% ± 5.0%	+37.9% ± 6.7%**	+32.6% ± 6.5%**
<i>unc-36(ad698)</i>	0.38 ± 0.04 Hz**	+14.5% ± 5.8%◇	+53.3% ± 11.0%**	+35.1% ± 8.0%**

Values are mean ± SEM; n varies by strain. Significance levels are determined using the Mann-Whitney rank sum test. All measurements were made on adult hermaphrodites in 1 mg/ml serotonin on hydrated 2% agarose pads. Diamonds indicate borderline significance (0.05 < p < 0.1). Single asterisks indicate moderate significance (0.005 < p < 0.05). Double asterisks indicate high significance (p < 0.005).

that rapid pumping requires input from pharyngeal neurons, while slow pumping can occur without neural input (very slow pumping in our assay appears to be a sign of impending death). To reduce the impact of alterations in neuronal behavior on our data, and to avoid an elevation of baseline ratio to a point at which calcium release rates became significant compared with calcium binding rates, we focused our analysis on the slow pumping behavior. Analysis of ratio traces indicated that rapidly pumping pharynxes exhibited a smaller ratio change per contraction than did slowly pumping pharynxes (Figure 4C). Likewise, the duration of the rising phase of the calcium transient was shorter during rapid pumping than during slow pumping (Figure 4D). However, the slope of the rising phase was independent of pumping rate (Figure 4E). Since the differences in the ratio increase between rapidly and slowly pumping pharynxes were proportional to the differences in duration, we concluded that they were simply a consequence of an extended duration of the calcium transient. To verify that the observed differences in rate and transient parameters were not both a consequence of varying sensitivity to serotonin, we applied both double and half normal concentrations of serotonin; no significant change in the trends for or values of any parameter was observed (data not shown). We thus were able to calculate mean values for pumping rate and transient parameters in wild-type worms (Table 1).

Mutations in the Calcium Channel Subunit EGL-19 Affect the Duration of Calcium Influx

The success of our characterization of wild-type worms motivated examination of calcium transients in mutants in the *egl-19* voltage-gated calcium channel. *egl-19* encodes the structural ($\alpha 1$) subunit of the pharyngeal voltage-gated calcium channel (Lee et al., 1997). Since the $\alpha 1$ subunit forms the pore of the channel, one would expect that mutations in *egl-19* could alter the duration or magnitude of calcium transients. *egl-19* null alleles are lethal, but both reduction-of-function and gain-of-function alleles have been identified in genetic screens (Trent et al., 1983; Avery, 1993; Lee et al., 1997). Electrical recordings from dissected mutant pharynxes have demonstrated that the gain-of-function alleles indeed cause extended depolarizations during muscle contraction, while loss-of-function alleles produce somewhat shortened depolarizations (Lee et al., 1997).

To aid comparison with previous electrophysiological results, we selected two gain-of-function alleles (*n2368* and *ad695*) and two reduction-of-function alleles (*n582* and *ad1006*) that had been previously characterized (Lee et al., 1997). Each allele was crossed into the *ljls1* background, and recordings were made using the same protocol as for the original *ljls1* strain. As shown in Figure 5 and Table 1, both *n2368* and *ad695* showed transients of increased duration. In fact, with the stronger allele, *n2368*, the transients frequently had an extended high-calcium plateau (Figure 5A, inset). Since the slopes of the transients were not greatly affected, the data suggest that the primary effect of the *n2368* and *ad695* mutant alleles is on the duration of the rising transient and/or the appearance of a plateau phase, and not on other aspects of the calcium influx. As expected, *ad1006* showed a decreased calcium transient duration without a drastic change in slope, consistent with a partial loss-of-function phenotype. The parameters for *n582* were statistically indistinguishable from those for wild type, suggesting that this mutation does not have a major effect on the calcium influx in the pharynx, although the mutation did decrease pumping rate (Table 1). Taken together, the close correspondence between our results and earlier electrical recordings supports the hypothesis that calcium is the major charge carrier during pharyngeal depolarization and suggests that calcium imaging can play a valuable role in the analysis of calcium channel function.

UNC-36 Voltage-Gated Calcium Channel $\alpha 2$ Subunit Implicated in Downregulation of Calcium Transients

Calcium channels in both vertebrates and *C. elegans* also contain a number of associated subunits that presumably are involved in dynamic regulation of the channel's activity or in static alteration of its properties. For example, all known calcium channels contain a large subunit called $\alpha 2$, a glycosylated integral membrane protein. The *unc-36* gene encodes a putative $\alpha 2$ subunit of pharyngeal calcium channels (Lee et al., 1997), and mutants defective in this gene have an observable pharyngeal pumping defect (Brenner, 1974; Avery, 1993). This suggests an important role for the UNC-36 protein in the pharynx, yet little is known about the role of the $\alpha 2$ subunit in the muscle cells of nematodes or other animals.

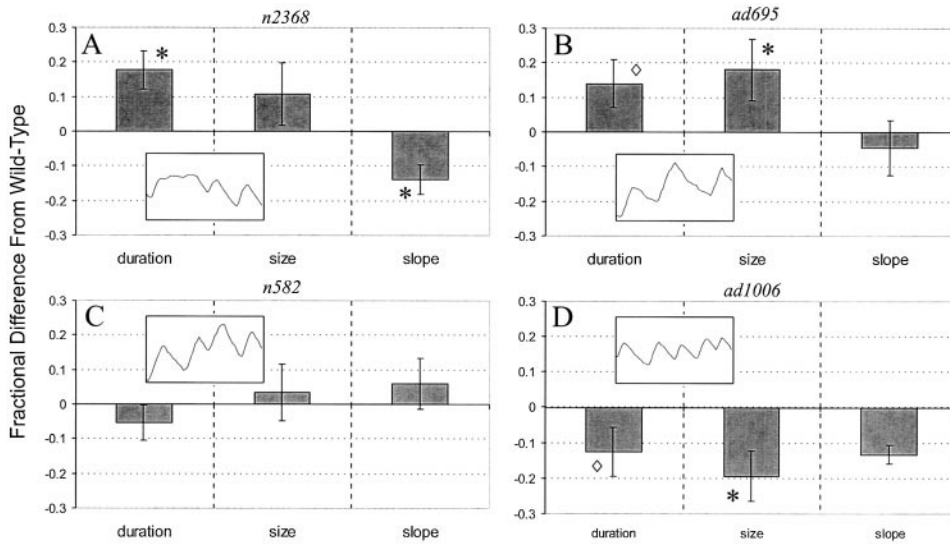


Figure 5. Altered Calcium Transients in *egl-19* Mutants

Comparison of mutants with wild type in worms pumping between 0.5 and 1.5 Hz. Graphs indicate percent difference from wild type for each parameter. Error bars indicate standard error of both mutant and wild type. Diamonds indicate possible differences from wild type ($0.05 < p < 0.10$). Asterisks indicate significant differences from wild type ($0.005 < p < 0.05$). Insets show 3 s of a sample trace; the vertical axis of the inset corresponds to a 12% ratio change.

(A) Gain-of-function mutant *n2368* shows transients of extended duration and diminished slope relative to wild type. The duration reflects the rising phase only and would be longer if calcium plateaus (inset) were included. The reduced slope may be an artifact of the arbitrary division made between rising and plateau phases.

(B) Gain-of-function mutant *ad695* shows transients of increased duration and total ratio increase; transient slope is not significantly different from that of wild type.

(C) Loss-of-function mutant *n582* shows no significant changes in transient parameters from wild-type worms.

(D) Loss-of-function mutant *ad1006* shows transients of decreased duration and size relative to wild type; the data do not have a parametric distribution, and hence the apparent decrease in slope is not statistically significant. As expected, the phenotype is opposite from the gain-of-function mutants.

To determine if *unc-36* mutations affect pharyngeal calcium transients, we constructed strains containing a mutant allele of *unc-36* and the *ljls1* integrated array. In the two different *unc-36* loss-of-function mutants analyzed (*e251* and *ad698*), the average rate of pumping was reduced relative to that of wild type (Table 1). Calcium imaging demonstrated that the *unc-36(e251)* allele caused a dramatic increase in the slope of the transients without altering their duration (Figure 6A). Likewise, the effect of allele *ad698* was to increase the slope without a major effect on duration (Figure 6B). To verify that the difference in slope was not caused by a difference in sensitivity of YC2.1 in an *unc-36* background, we measured the dynamic range ofameleon in the *e251* background; an example trace is shown in Figure 6C. No difference between N2 and *e251* was detected in the dynamic range (Figure 6D), indicating that the difference in slopes was not due to a higher proportion of inactiveameleon in the *unc-36* background. There also was no difference between baseline ratios (1.410 ± 0.020 for N2, 1.436 ± 0.029 for *e251*), which indicates that the difference is not due to increased responsiveness caused by a greater proportion of calcium-free indicator at baseline in *e251*. Although we cannot rule out an *unc-36* background altering endogenous buffers—such that free calcium during calcium influx is elevated, even though the influx itself is normal—since *unc-36* is a calcium channel subunit, the most parsimonious explanation is that the effect is on calcium influx itself. Thus,

our imaging experiments indicate that loss of *unc-36* function leads to an increase in the magnitude of pharyngeal calcium transients and suggests that the $\alpha 2$ subunit of the calcium channel might function to negatively regulate the calcium flux into the pharynx.

Discussion

Cameleon Is a Viable Sensor for Investigating Muscle Cell Physiology In Vivo

We have shown that ectopically expressedameleon can be used to detect and measure calcium transients in the pharynx of live *C. elegans*. These transients are reliably detected, and parameters describing both the duration and level of elevated calcium can be calculated for worms of a given strain. Furthermore, we have shown that this method is sufficiently sensitive to identify mutants that display calcium dynamics measurably different from those of wild-type worms.

In addition to the pharyngeal muscle, *C. elegans* contains a number of specialized muscle groups, each dedicated to a particular behavior. In the hermaphrodite, these include the body wall muscles (involved in locomotion), the defecation muscles (involved in defecation), the oviduct muscles (involved in ovulation), and the vulval muscles (involved in egg laying) (White, 1988). The functional activities of these muscle groups are known to be regulated by a diverse array of neuromodulators.

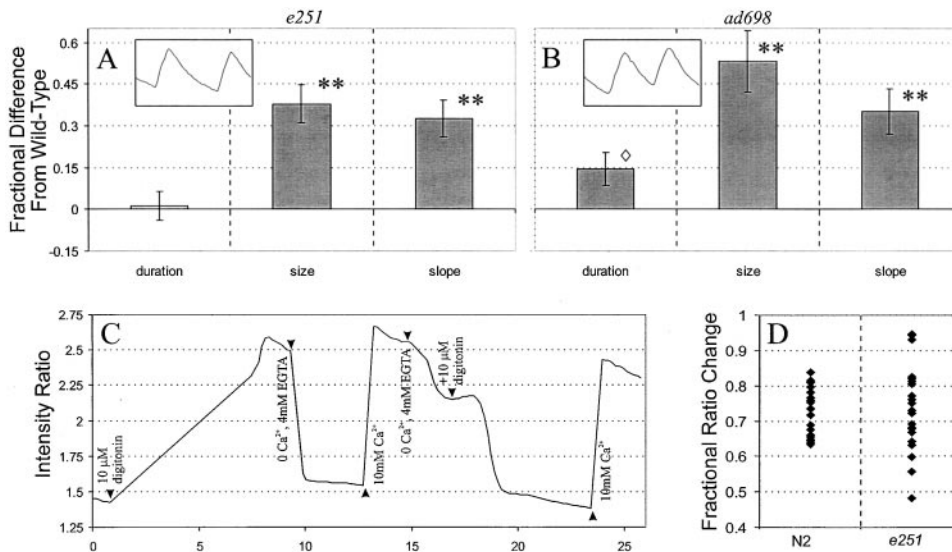


Figure 6. *unc-36* Mutants Show Larger Calcium Influx

Comparison of mutants with wild type in worms pumping between 0.5 and 1.5 Hz. Graphs indicate percent difference from wild type for each parameter. Error bars indicate standard error of both mutant and wild type. Double asterisks indicate highly significant differences from wild type ($p < 0.005$). Single asterisks indicate significance ($0.005 < p < 0.05$). Diamonds indicate possible significance ($0.05 < p < 0.10$). (A) Allele *e251* shows markedly larger transients than do wild-type worms ($p < 0.005$), without a corresponding change in the duration of contractions. Inset shows a sample trace (horizontal length is 3 s; vertical length is 12% ratio change). (B) Allele *ad698* likewise shows larger transients ($p < 0.005$) and slope ($p < 0.005$), with a possible smaller increase in duration of contractions ($0.05 < p < 0.10$). Inset shows a sample trace (horizontal length is 3 s; vertical length is 12% ratio change). (C) Control verifying that cameleon is functioning properly in the *e251* background. A dissected head is exposed to digitonin and placed alternately in solutions of 10 mM Ca^{2+} or 0 Ca^{2+} + 4 mM EGTA to determine maximal and minimal fluorescence ratio. An example trace is shown; over five worms, the maximal ratio was a mean of $73\% \pm 11\%$ over the minimal ratio. Arrowheads indicate solution changes. (D) Comparison of control maximal/minimal ratios for wild type and *e251*. Each dot indicates one maximum/minimum ratio measurement. Left column is wild type, right is *e251*. The observed pattern is inconsistent with *e251* having a 30% larger response than do wild type ($p < 0.01$).

Moreover, a large number of mutants have been described that affect these various behaviors, and the genes defined by these mutations encode potential components of signaling pathways that might regulate muscle excitation and/or contraction. Calcium imaging using cameleon provides a powerful tool for distinguishing mutants that affect calcium influx from those that affect contractile duration without otherwise altering calcium dynamics and from those that have normal calcium dynamics but abnormal contraction. Using this technique, it should therefore be possible to identify genes whose products regulate calcium channel activity in muscles and to study their effects *in vivo*, and thereby gain insight into the mechanisms of calcium channel regulation.

Insights into the Function of Calcium Channel Subunits

We determined that mutations affecting two subunits of the pharyngeal voltage-sensitive calcium channel altered the dynamics of calcium influx during feeding. Mutations in *egl-19*, which encodes the $\alpha 1$ subunit, affected the duration of the calcium transient without having other major effects on the calcium influx. The duration increases in gain-of-function alleles *n2368* and *ad695* are consistent with prior electrical recordings (Lee et al., 1997), as is the duration decrease in loss-of-function allele *ad1006*. The loss-of-function allele *n582*, which has subtle electrical defects and visually appears

to have “weak” contractions, did not appear to have calcium transients significantly different from those of wild type, despite a decreased average pumping rate. It is possible that *n582* does have a physiologically important effect on calcium in the pharynx but that the change was below our ability to detect. Alternatively, the mutation may affect the activation potential of the channel or otherwise affect excitability. Analysis of other alleles, preferably using both calcium imaging and electrical techniques, may provide insight into the relationship between the structure of $\alpha 1$ subunits and their activity.

Analysis of mutants in *unc-36* also provided an interesting insight into the possible function of the $\alpha 2$ subunit. *unc-36* mutants show two visible abnormalities in feeding behavior (Avery, 1993). First, in contrast to wild type, *unc-36* mutants are unable to pump at high frequency in the presence of food or serotonin. Since neuronal input is required for rapid pumping, and since many mutants with specific defects in fast pumping are known to be deficient in synaptic transmission, this aspect of the *unc-36* feeding phenotype is probably due to a lack of neuronal *unc-36* function. Second, *unc-36* mutants also exhibit an abnormality in the pattern of pharyngeal muscle contraction, a phenotype known as the “slippery pharynx.” Since the slippery pharynx is not a hallmark of synaptic transmission mutants, and since GFP reporters indicate that *unc-36* is expressed in the pharynx itself (T. Tam and W. R. S., unpublished data),

it is logical to suppose that this phenotype results from a defect in the muscle itself. However, the visible phenotype of *unc-36* provided little insight into how it might affect the activity of calcium channels in the pharyngeal muscle. Cameleon imaging showed that loss-of-function alleles of *unc-36* caused increased calcium influx. This indicated that the $\alpha 2$ subunit directly or indirectly functioned as a negative regulator of calcium influx in the pharynx. Potentially, UNC-36 could physically affect the $\alpha 1$ subunit and be a site of regulation itself. Alternatively, it could interact with negative regulators that acted on the $\alpha 1$ subunit, or it could be required for proper localization or increased turnover of the channel complex. Overexpression studies in *Xenopus* oocytes and vertebrate cell culture have shown that the $\alpha 2$ subunit increases both the conductance and the rate of inactivation of coexpressed $\alpha 1$ channels, especially when the β subunit is coexpressed (Singer et al., 1991; De Waard and Campbell, 1995; Bangalore et al., 1996). Our results are consistent with an inactivation defect that leads to increased calcium influx, though we saw no evidence for decreased conductance. Although more work would be needed to distinguish between these and other possibilities, this finding illustrates the benefit of calcium imaging, as there was no way to infer the effect of this protein on calcium dynamics from its behavioral phenotype alone.

Technical Considerations for Calcium Imaging with Cameleon

Our experimentation with different imaging systems provided a number of lessons about the technical requirements for cameleon imaging in behaving organisms in which calcium changes occur rapidly. Perhaps the most important aspect of an effective system is the ability to perform video rate ratiometric imaging. The susceptibility of the individual wavelength traces to movement artifacts and photobleaching makes it critical to obtain simultaneous measurements of both emission wavelengths at a speed adequate to detect relatively brief events. An emission splitter as used here, unlike a filter wheel system, records the two images simultaneously on a single CCD at the full frame rate of the camera, although the field of view is reduced 2-fold. Video rate confocal and two-photon microscopes with nonimaging detectors (Tsien and Bacskaï, 1995; Fan et al., 1999) are important alternatives to split emission CCDs and provide the advantages of optical sectioning, stroboscopic illumination, and inherent registration of the two emission wavelengths. Preliminary trials with video rate two-photon excitation microscopes showed pharyngeal calcium transients similar to those characterized here, but the CCD system proved more reliable and better in signal-to-noise ratio, with less photobleaching, probably because the wide-field observation could collect more photons from a greater thickness of sample volume. In our very transparent preparation, targeted gene expression already restricted the cameleon quite accurately to the tissue of interest, so the optical sectioning capability of confocal or two-photon imaging was unnecessary or even counterproductive for maximizing photon collection. The ability of two-photon excitation to confine photobleaching to just the plane of focus was of little value

when that plane was being observed constantly and when diffusion of unbleached indicator molecules from other planes was probably quite slow, as expected for a ~ 70 kDa protein. However, many other preparations and biological questions will still require confocal or two-photon excitation instruments.

Prospects for Using Cameleon in Other Cell Types

Calcium imaging using cameleon is in principle applicable to a wide variety of tissues in *C. elegans*. For example, intestinal cells, which are neither muscular nor neuronal, have recently been implicated in control of the periodic defecation of the worm (Dal Santo et al., 1999). Transient increases in calcium were observed in intestinal cells injected with fura-2; these transients preceded the first defecation-related muscle contractions. However, due to the technically challenging nature of the injection procedure, it was only possible to inject and image from a single intestinal cell in each animal. Intestinal expression of cameleon would allow transients to be monitored over the entire length of the intestine simultaneously, which would help determine the nature of spatial coordination of intestinal calcium transients. Also, avoiding the step of single cell injection would greatly facilitate the analysis of the calcium transient phenotype of known defecation-defective mutants. Since the intestine is comparable in size to the pharynx, has several strong cell type-specific promoters, and is known to undergo robust calcium transients, cameleon imaging should be possible in this tissue without substantial modification to the methods described here.

We found that electrical stimulation could reliably induce visible ratio changes in neurons. Thus, it should be possible to use cameleon-based calcium imaging to study voltage-gated calcium channel function in neurons, as we have begun to do in the pharynx. Moreover, if a single neuron were driven electrically, the response of its synaptic partners could be recorded to begin building a map of functional connectivity to complement the known physical connectivity (White et al., 1986). This approach would also allow noise to be averaged out over multiple trials and could enhance comparisons between small ratio changes. The ability to simultaneously monitor the activity of multiple identified neurons in an intact behaving animal would be enormously useful for understanding the cellular basis of behavior. Existing protocols for recording electrically from *C. elegans* neurons involve slicing open or rupturing the cuticle to expose a cell of interest, so an electrical alternative is not immediately obvious. Electrophysiology in *C. elegans* and another nematode, *Ascaris*, indicate that calcium is the main carrier of inward positive current (Davis and Stretton, 1989; Goodman et al., 1998), and the *C. elegans* genome contains no recognizable voltage-gated sodium channels (Bargmann, 1998; *C. elegans* Sequencing Consortium, 1998). Thus, there is little doubt that neuronal calcium transients are ubiquitous in *C. elegans*. Since neuronal cell bodies in *C. elegans* are small (~ 2 μm diameter), in vivo recordings from neurons are more difficult to obtain than muscle recordings due to increased sensitivity to movement and background noise. Nonetheless, neuronal activity in response to the application of a stimulus—an odorant or neurotransmitter,

for instance—should be detectable without major modifications to the protocol used here. Additionally, with further optimizations to the imaging equipment, protein expression levels, and recording protocols, detection of neuronal calcium transients in intact *C. elegans* may be practical, even in the absence of pairing with a stimulus.

Although *C. elegans* is particularly suited to cameleon imaging due to its transparency and facile genetics, this method may be useful in other organisms, as well. For example, *Drosophila* has equally powerful genetics and an even more diverse set of cell type-specific promoters to direct localized cameleon expression. Moreover, although still relatively small, the neurons of *Drosophila* are somewhat larger and may contain larger calcium transients than do the neurons of *C. elegans*. While the opaque exoskeleton of *Drosophila* may make imaging from intact adult animals difficult, existing methods for recording from larvae should be applicable, and strong promoters may facilitate imaging in all developmental stages (Sun et al., 1999). Other genetically manipulable organisms, such as mouse, present their own set of challenges, as well as potential advantages, for use of cameleon in imaging studies. Further modification of the methods described here should make it possible to overcome these species-specific challenges and realize the prospective power of genetically encoded sensors as probes for nervous system function.

Experimental Procedures

Construction of Cameleon Expression Plasmids

A pharyngeal specific expression vector was constructed using the backbone of the Fire Lab '97 Vector Kit plasmid L3613, the promoter sequence of the *myo-2* gene, and the coding sequence of either YC2.1 or YC3.1. Restriction sites BamHI and EcoRI were used to remove the existing promoter and coding sequence from L3613. PCR was used to amplify the *myo-2* promoter from *C. elegans* genomic DNA using primers 5'-GGATCCGAGGCATTGAATTGGGGTGG TGG-3' and 5'-AAGCTTCTGTGTCGACGATCGAGGG-3', corresponding to 1170 base pairs upstream of the translation start site, and sufficient for pharyngeal specific expression, according to Okkema et al. (1993). Primers include a 5' BamHI site and a 3' HindIII site. The cameleon coding sequence was removed using HindIII and EcoRI, and the cameleon, promoter, and backbone fragments were ligated to produce the final expression vector. A neuronal specific expression vector was constructed in the same manner. PCR was used to amplify 2355 base pairs upstream of the *unc-119* translation start site; the primers used were 5'-GGATCCCTTGG GAAAAACGGGCG-3' and 5'-GCTCTGCCTCATATAAGCTTTTGTG TCTG-3'.

Construction of Transformed Strain of *C. elegans* Carrying Cameleon Expression Plasmid

Purified plasmid DNA of the pharyngeal expression vector was injected into *dpy-20(e1282ts)* worms along with a coinjection marker plasmid carrying the *dpy-20(+)* gene, according to the protocol in Mello and Fire (1995), to obtain a strain carrying the expression vector on an extrachromosomal array. The strain carrying YC2.1 was then subjected to γ -ray irradiation, as outlined in Mello and Fire (1995; p. 467), to generate a strain carrying an intrachromosomal array. Two independent integrants were obtained. Both showed strong tissue-specific expression of the protein; one of the two (*ljIs1*) was used for all crosses. The neuronal expression vector was introduced similarly, but not irradiated, to give an intrachromosomal array, generating the extrachromosomal array *ljEx3*.

Optical Recordings

Optical recordings were performed on a Zeiss Axioskop with a Pentamax EEV 512 \times 1024 CCD camera (Princeton Instruments). A

MultiViewer emission image splitter (Princeton Instruments) was used to display two wavelengths simultaneously on the single CCD chip. Recordings were made on a 100 MHz Pentium running MetaFluor 3.6 (Universal Imaging) under Windows 95. A 40 \times water immersion objective (Olympus) was used for all recordings. For most recordings, 50 ms/frame exposures were taken with 4 \times 4 binning. Image stacks were occasionally converted to ratio pairs for visual inspection using the PI MultiViewer plug in for MetaFluor. Fluorescence ratio measurements were made using custom software described below. Filter/dichroic sets consisted of excitation (405 nm, 40 nm bandwidth), cyan emission (483 nm, 25 nm bandwidth), yellow emission (535 nm, 25 nm bandwidth), and 510 nm dichroic mirrors.

Dissected Head Sample Preparation and Recording

Individual worms were transferred to a dried agarose pad on a coverslip to immobilize them and were covered with halocarbon oil to prevent dehydration. A razor was used to sever the head just posterior to the pharynx, exposing the pharynx to external solutions. The severed head was skewered through the cuticle using a glass microinjection needle and transferred to *C. elegans* intracellular saline solution containing 136.5 mM potassium gluconate, 17.5 mM potassium chloride, 9.0 mM sodium chloride, 1.0 mM magnesium chloride, and 10 mM HEPES (pH 7.2) (Avery et al., 1995). An initial application of 20 μ M digitonin was used to provide intracellular access; the bath solution was then switched repeatedly between intracellular saline with 0 Ca^{2+} + 4 mM EGTA and 10 mM Ca^{2+} . Images were taken at 0.1 Hz during these experiments; solutions were switched after the ratio had reached a plateau. Occasional reapplication of digitonin was needed to maintain good intracellular access. Analysis was performed online in MetaFluor by measuring the fluorescent intensity of each wavelength over the terminal bulb of the pharynx. After recording was complete, the image stack was analyzed with the custom measurement software described below.

Whole Worm Sample Preparation and Recording

Six to ten worms were transferred to a hydrated 2% agarose pad in M9 solution with 1 mg/ml serotonin and partially immobilized by using a drawn capillary tube to dot cyanoacrylate glue on or near their tails. An additional 5 μ l of 1 mg/ml serotonin in M9 was added to keep the sample hydrated during recordings and to induce pharyngeal pumping (Avery and Horvitz, 1990). Worms whose heads or entire bodies were accidentally mired in glue were not used in the recordings. In most cases, two worms were recorded from each pad. Each pharyngeal recording consisted of 20 10 s image streams at 20 Hz, taken 1 min apart. This protocol allowed sufficient time (50 s) for the images that had been streamed to RAM to be stored on the computer hard drive. Neuronal recordings ranged from 3 to 5 s/neuron, with several widely separated neurons imaged in each worm; sample preparations were otherwise identical.

Electrical Stimulation of *C. elegans* Neurons

Worms were glued to 2% agarose pads, without serotonin, as previously described. It was necessary to apply glue more liberally in order to immobilize the worm sufficiently. The worm and pad were then immersed in Dent's saline (Avery et al., 1995). A standard silver chloride glass electrode, pulled to a tip diameter of \sim 0.5 μ m, was used to puncture the worm's cuticle on the side of the head; the tip was then located near the center of the nerve ring but was not embedded in the pharyngeal muscle. Current (0.3 mA) was applied through an Isoflex isolation unit (AMPI) driven by a Master 8 multi-channel pulse generator (AMPI). Fluorescent recordings were made as described previously. The bleaching rate for the YFP component of the signal was \sim 10% over a 20 s recording. Since the changes were only a few percent, this bleaching made visualization difficult, although it did not affect the ability to detect transients. We therefore removed the exponential trend, as measured by fitting a single exponential to the prestimulus and poststimulus portions of the trace. The CFP component was not affected significantly by bleaching, but FRET was reduced somewhat due to YFP bleaching, causing a slight upward trend, which we removed for ease of visualization using the same method.

Automated Extraction of Mean Fluorescence Ratio from Image Series

To facilitate the rapid analysis of large numbers of image stacks, a command line Windows 95 program was designed that extracts the mean fluorescence ratio from each frame in the stack. The fundamental operation of the program is to locate the center of the target tissue with subpixel accuracy. In the case of the pharynx, which was unambiguously the brightest object in the field of view, an approximate location was determined using that criterion. For neuronal data, the approximate initial position of each neuron of interest was specified by hand. The exact position is then computed iteratively by computing the intensity-weighted center of a region of interest large enough to encompass the target tissue and updating the region center if the intensity-weighted center differs significantly from the region center. The optical splitting of the two wavelengths does not produce a perfect bisection of the CCD array and can change slightly from day to day. Therefore, the program has the ability to compute the mean difference in position between two regions of interest and to use that difference to determine the offset between the two wavelength images. Once an offset is specified, for each frame in the stack the center of the tissue of interest can be computed as described above. A single region of interest is used for the neuronal recordings, while a series of concentric circles are taken about the center of the pharynx; average intensity is measured for each and output to a log file. The smallest circle entirely containing the pharynx (judged by recording noise, which is reduced when the circle does not intersect the pharynx) was used for further analysis; this usually corresponded to a radius of 11 pixels. Optimal region size for neurons was determined by hand. Subpixel resolution is achieved by interpolating between adjacent pixels; this prevents excessive noise from single pixels flickering in and out of the region of interest from frame to frame.

Detection and Measurement of Transients in Fluorescence Ratio

The numerical computation and matrix manipulation program GNU Octave, an open source clone of MATLAB (The MathWorks), was used for all data processing. The intensity was the ratio from the average intensity log file described above; then, the derivative of the ratio was calculated and smoothed by using an 8 Hz triangular window. With 20 Hz data, this turned out to be equivalent to averaging adjacent measurements. Empirically, transient rises in calcium accompanying pharyngeal contraction were observed to last at least 100 ms and to have a rate of rise of at least 5%/s. Smaller transients would have been difficult to distinguish from noise by eye, and automatic detection of transients using the 5%/s criteria seemed as reliable as making measurements by eye. One exception was in mutants with very extended contractions; for those, only the initial rise was detected, not the extended elevated plateau. The entire transient was considered to be all frames surrounding the triggering frames (two adjacent rises of at least 5%/s) that either showed an increase in ratio themselves or were immediately between rises of at least 5%/s. The duration, maximum increase, and slope of each transient were recorded. Duration was considered to be (frame rate) * (number of frames in transient - 1). Maximum increase was calculated as (highest ratio in transient) - (lowest ratio in transient). Slope was calculated by a least-squares fit to the trace during the transient.

Statistical Analysis of Recording Parameters

Variation in the three parameters measured for each transient was observed from transient to transient, trace to trace, and worm to worm within the same train. Worm behavior—the average rate of pumping—was observed to change in many cases over the duration of the 20 min recordings. However, within each 10 s recording stream, behavior seemed fairly stable. Therefore, mean duration, increase, and slope of transients were calculated for each 10 s stream. Since there was worm-to-worm variation, statistical comparison had to be at the worm level. Since the parameters were affected by the worm's pumping rate, only streams with the appropriate pumping rate (0.5–1.5 Hz) were considered. Further, when wild-type and mutant worms were compared, streams were excluded until both data sets contained the same number of streams at each frequency. The resulting rank-normalized streams were then

averaged worm by worm. The values for the wild-type worms and those for that mutant strain were compared for statistically significant differences by using the nonparametric Mann-Whitney rank sum test. One should note that since multiple comparisons were made with wild type, a result of $p < 0.05$ is valid only for the exact comparison being made. If the data were to be treated as a survey of mutants to catalog which were different from wild type, the nonparametric Dunnett's test should be used instead. The Mann-Whitney test was used for simplicity, but as with any pairwise test, if there are enough comparisons a result of $p < 0.05$ occurring somewhere would be expected by chance. To calculate mean values and parametric deviations for each strain, mutant data were normalized for pumping rate against wild type as described above. The mean and standard error for each worm were calculated, and then the results for each worm were used to calculate the mean for the strain. Error was taken to be the standard error on the average over the worms, plus the error propagated from each worm using the standard formula for propagation of error.

Kinetic Measurements of Cameleon

Solutions containing 10 mM Tris, 500 μ M Ca^{2+} , and 5 μ M YC2.1 or YC3.1 (pH 8) were mixed with equal volumes of 10 mM Tris, 4 mM EDTA (pH 8) using a stop-flow fluorimeter (Applied Photophysics). Fluorescence intensity in cyan and yellow wavelengths was measured in separate experiments using an excitation monochromator at 405 nm (5 nm bandwidth) in each case, and 483 nm (25 nm bandwidth) and 535 nm (25 nm bandwidth) emission filters for cyan and yellow, respectively. The sampling rate was 2 kHz for the first 200 data points (100 ms) and 200 Hz for an additional 200 data points (1000 ms). Curve fitting to determine relaxation times was performed on the software package SigmaPlot (Jandel Scientific).

Acknowledgments

We are grateful to Mark Ellisman for the use of his video rate two-photon microscope for neuronal imaging, to Gary Fan for assistance in using it, and to Joseph Adams for the use of his stop-flow fluorimeter to analyze the in vitro kinetics of cameleon. We also thank Leon Avery and the *Caenorhabditis* Genetics Center for strains, and Tim Yu and members of our laboratories for discussions. This work was supported by grants from the National Science Foundation (IBN-9723250), the National Institutes of Health (DA11556), the Esther A. and Joseph Klingenstein Foundation, the Alfred P. Sloan Foundation, and the Arnold and Mabel Beckman Foundation (to W. R. S.); predoctoral training grants from the Markey Foundation and the National Institutes of Health (to R. K.); and grants from the National Institutes of Health (NS27177) and the Howard Hughes Medical Institute (to R. Y. T.).

Received January 19, 2000; revised May 24, 2000.

References

- Avery, L. (1993). The genetics of feeding in *Caenorhabditis elegans*. *Genetics* 133, 897–917.
- Avery, L., and Horvitz, H.R. (1989). Pharyngeal pumping continues after laser killing of the pharyngeal nervous system of *C. elegans*. *Neuron* 3, 473–485.
- Avery, L., and Horvitz, H.R. (1990). Effects of starvation and neuroactive drugs on feeding in *Caenorhabditis elegans*. *J. Exp. Zool.* 253, 263–270.
- Avery, L., and Thomas, J.H. (1997). Feeding and defecation. In *C. elegans II*, D.L. Riddle et al., eds. (Cold Spring Harbor, NY: Cold Spring Harbor Laboratory Press), pp. 679–716.
- Avery, L., Raizen, D., and Lockery, S. (1995). Electrophysiological methods. In *Caenorhabditis elegans: Modern Biological Analysis of an Organism*, Methods in Cell Biology, Volume 48, H.F. Epstein and D.C. Shakes, eds. (San Diego, CA: Academic Press), pp. 251–269.
- Bangalore, R., Mehrke, G., Gingrich, K., Hofmann, F., and Kass, R.S. (1996). Influence of L-type Ca channel $\alpha_1\delta$ -subunit on ionic and gating current in transiently transfected HEK 293 cells. *Am. J. Physiol.* 270, H1521–H1528.

- Bargmann, C. (1998). Neurobiology of the *Caenorhabditis elegans* genome. *Science* 282, 2028–2033.
- Brenner, S. (1974). The genetics of *Caenorhabditis elegans*. *Genetics* 77, 71–94.
- C. elegans* Sequencing Consortium (1998). Genome sequence of the nematode *C. elegans*: a platform for investigating biology. *Science* 282, 2012–2018.
- Dal Santo, P., Logan, M.A., Chisholm, A.D., and Jorgensen, E.M. (1999). The inositol trisphosphate receptor regulates a 50-second behavioral rhythm in *C. elegans*. *Cell* 98, 757–767.
- Davis, R.E., and Stretton, A.O. (1989). Passive membrane properties of motorneurons and their role in long-distance signalling in the nematode *Ascaris*. *J. Neurosci.* 9, 403–414.
- De Waard, M., and Campbell, K.P. (1995). Subunit regulation of the neuronal α_{1A} Ca^{2+} channel expressed in *Xenopus* oocytes. *J. Physiol.* 485, 619–634.
- Fan, G.Y., Fujisaki, H., Miyawaki, A., Tsay, R.-K., Tsien, R.Y., and Ellisman, M.H. (1999). Video-rate scanning two-photon excitation fluorescence microscopy and ratio imaging with cameleons. *Biophys. J.* 76, 2412–2420.
- Goodman, M.B., Hall, D.H., Avery, L., and Lockery, S.R. (1998). Active currents regulate sensitivity and dynamic range in *C. elegans* neurons. *Neuron* 20, 763–772.
- Lee, R.Y.N., Lobel, L., Hengartner, M., Horvitz, H.R., and Avery, L. (1997). Mutations in the $\alpha 1$ subunit of an L-type voltage-activated Ca^{2+} channel cause myotonia in *Caenorhabditis elegans*. *EMBO J.* 16, 6066–6076.
- Maduro, M., and Pilgrim, D. (1995). Identification and cloning of *unc-119*, a gene expressed in the *Caenorhabditis elegans* nervous system. *Genetics* 141, 977–988.
- Mello, C., and Fire, A. (1995). DNA transformation. In *Caenorhabditis elegans: Modern Biological Analysis of an Organism*, Methods in Cell Biology, Volume 48, H.F. Epstein and D.C. Shakes, eds. (San Diego, CA: Academic Press), pp. 451–482.
- Miyawaki, A., Llopis, J., Heim, R., McCaffery, J.M., Adams, J.A., Ikura, M., and Tsien, R.Y. (1997). Fluorescent indicators for Ca^{2+} based on green fluorescent proteins and calmodulin. *Nature* 388, 882–887.
- Miyawaki, A., Griesbeck, O., Heim, R., and Tsien, R.Y. (1999). Dynamic and quantitative Ca^{2+} measurements using improved cameleons. *Proc. Natl. Acad. Sci. USA* 96, 2135–2140.
- Okkema, P.G., Harrison, S.W., Plunger, V., Aryana, A., and Fire, A. (1993). Sequence requirements for myosin gene expression and regulation in *Caenorhabditis elegans*. *Genetics* 135, 385–404.
- Raizen, D.M., Lee, R.Y.N., and Avery, L. (1995). Interacting genes required for pharyngeal excitation by motor neuron MC in *Caenorhabditis elegans*. *Genetics* 141, 1365–1382.
- Singer, D., Biel, M., Lotan, I., Flockerzi, V., Hofmann, F., and Dascal, N. (1991). The roles of the subunits in the function of the calcium channel. *Science* 253, 1553–1557.
- Sun, B., Peizhang, X., and Salvaterra, P.M. (1999). Dynamic visualization of nervous system in live *Drosophila*. *Proc. Natl. Acad. Sci. USA* 96, 10438–10443.
- Trent, C., Tsung, N., and Horvitz, H.R. (1983). Egg-laying defective mutants of the nematode *Caenorhabditis elegans*. *Genetics* 104, 619–647.
- Tsien, R.Y., and Bacsikai, B.J. (1995). Video rate confocal microscopy. In *Handbook of Biological Confocal Microscopy*, Second Edition, J.B. Pawley, ed. (New York: Plenum Press), pp. 459–478.
- White, J. (1988). The anatomy. In *The Nematode Caenorhabditis elegans*, W.B. Wood, ed. (Cold Spring Harbor, NY: Cold Spring Harbor Laboratory Press), pp. 81–122.
- White, J.G., Southgate, E., Thomson, J.N., and Brenner, S. (1986). The structure of the nervous system of the nematode *Caenorhabditis elegans*. *Philos. Trans. R. Soc. Lond. B Biol. Sci.* 314, 1–340.